Interactions between an Alkylamine-Terminated Perfluoropolyether and the Amorphous Hydrogenated Carbon Surface

R. J. Waltman

Hitachi Global Storage Technology, 5600 Cottle Road, San Jose, California 95193

Received July 1, 2003

The bonding of molecularly thin (10 Å) dipropylamine-terminated ZDPA 4000 and the hydroxyl-terminated Zdol 4000 lubricant films to amorphous hydrogenated carbon (CHx) are compared from 20 to 150 °C. The kinetic results demonstrate that the rate at which both ZDPA 4000 and Zdol 4000 bond to CHx is nonclassical with a time-dependent rate coefficient that is best described by the general form: $k(t) \propto k_B t^{-h}$. For ZDPA, the bonding rate coefficient is observed to scale as $t^{-0.25}$ while for Zdol the bonding rate coefficient is observed to scale as t^{-1}. The $t^{-0.25}$ bonding rate is shown to be consistent with diffusion-limited kinetics that originate from a high density of ZDPA−CHx reactant pairs that leads to a segregation of reactant pairs, while the t^{-1} bonding rate results when bonding occurs from a more liquidlike (no segregation) Zdol film structure. Surface energy measurements are indicative of initial intermolecular interactions between the dipropylamine end groups and the CHx surface despite a low bonded fraction. These results indicate that the lubricant end group can profoundly dictate the physical state of the confined lubricant films on the CHx surface. The kinetic studies are accompanied by both experimental data and ab initio calculations on possible bonding interactions between the lubricant end groups and possible CHx surface functional moieties. Infrared sprectroscopy is used to show that the ZDPA end group, in the presence of carboxylic acid, is capable of forming the $NH^+-{}^-OOC$ salt as characterized by an intense absorption band at 1673 cm^{-1}. H-bond energies for ZDPA−CHx(−OH) and Zdol−CHx(−OH) dimers are computed to be −5.3 and −4.4 kcal/mol, respectively. The energetics of the dimer interactions are discussed within the context of the observed lubricant bonding and debonding kinetics.

Introduction

The storage density of hard disk drives have increased at a rate of ∼60% during the past decade. The increase has been achieved by the implementation of advanced magnetic alloys and sensor technologies and by significant reduction of the physical spacing between the flying read−write head and the magnetic recording disk. Data rates (latency, access time, and internal data rate) have also been improved by increasing the disk rotational velocity. However, both low-flying and higher disk velocities are placing stringent demands on the tribological properties of the protective, wear-resisting films utilized at the head−disk interface (HDI). Foremost among these is the increased number of intermittent contacts between the head and the disk surface, which is necessitating the use of thinner, lower molecular weight lubricant films to provide increased clearance[1,2] and more highly bonded lubricant films to reduce lubricant loss from the disk surface.[3] A possible concern in the limit of continuous contact could be the reduced mobility and hence the reduced durability of such lubricant films.[4−6]

As alluded to above, the lubricant itself can mediate head−disk contact in low-flying hard-disk drives. Therefore, the choice of lubricant structure, molecular weight, and film thickness are significant determinants of tribological reliability in the hard-disk drive affecting slider−disk clearance,[1,2] lubricant film thickness uniformity,[3] and HDI durability.[4−7] Perfluoropolyether (PFPE) lubricants based upon a copolymer of perfluoromethylene oxide and perfluoroethylene oxide monomer units, capped by hydroxyl groups, continue to be widely used in these applications and are commercially available as Fomblin Zdol (Figure 1), Zdol-TX, and Z-Tetraol. The piperonyl-terminated Fomblin AM-3001 is often used in lubricant systems employing the cyclotriphosphazene-based additive due to their greater mutual solubility.[8] Cyclotriphosphazene-terminated perfluoropolyether lubricants are also commercially available.[9] PFPE lubricants functionalized by a variety of

(1) Khurshudov, A.; Waltman, R. J. *Tribol. Lett.* **2001**, *11*, 143.
(2) Waltman, R. J.; Khurshudov, A. *Tribol. Lett.* **2002**, *13*, 197.
(3) Waltman, R. J.; Tyndall, G. W. *J. Magn. Soc. Jpn.* **2002**, *26*, 97.
(4) Karis, T. E.; Tyndall, G. W.; Waltman, R. J. *Tribol. Trans.* **2001**, *44*, 249.
(5) Wang, R.-H.; White, R. L.; Meeks, S. W.; Min, B. G.; Kellock, A.; Homola, A.; Yoon, D. *IEEE Trans. Magn.* **1996**, *32*, 3777.
(6) Min, B. G.; Choi, J. W.; Brown, H. R.; Yoon, D. Y.; O'Connor, T. M.; Jhon, M. S. *Tribol. Lett.* **1995**, *1*, 225.
(7) Chen, C.-Y.; Bogy, D. B.; Cheng, T.; Bhatia, C. S. *IEEE Trans. Magn.* **2000** *36*, 2708.
(8) Jiaa, C. L.; Liu, Y. *Tribol. Lett.* **1999**, *7*, 11.
(9) Matsumura Oil Research Corporation, Kobe-City, Japan. URL: http://www.moresco.co.jp/ and e-mail: hirasawa@moresco.co.jp.

10.1021/cm030065b CCC: $27.50
Published on Web 12/13/2003

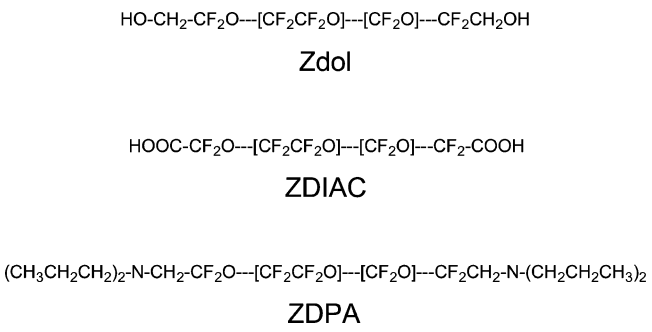

Figure 1. Chemical structures of the lubricants used in these studies.

other end groups including amine, alkylamine, nitrile, and epoxide have also been proposed for use on rigid magnetic disks.[10,11]

Recently, a perfluoropolyether lubricant terminated on the chain ends by a dialkylamine (Figure 1) has been proclaimed to be "ultrastable," providing increased resistance to catalytically induced chemical degradation and superior contact start−stop (CSS) durability.[12] It is empirically established that the CSS durability of thin film disks is a strong function of the lubricant film thickness and bonded fraction.[4,5] Moreover, since the bonded fraction can increase with the time after which the lubricant is applied to the disk surface,[13] the expectation is that the CSS durability as evaluated on a spin-stand could also be time-dependent. Therefore, the connection between lubricant parameters and the results of a CSS durability test can only be made when both the film thickness and the bonded fraction are known quantities at the time of the test. Thus, knowledge of the lubricant bonding kinetics is a crucial parameter of tribological reliability and represents the motivation for the current work.

In this report, we present the bonding kinetics of a molecularly thin (10 Å) dipropylamine-terminated perfluoropolyether, referred to as "ZDPA", Figure 1, on the CHx amorphous hydrogenated carbon surface. The kinetic experiments are conducted to probe the time dependence of the bonding reaction and the degree of confinement of the "liquid" films on the CHx surface. It has been shown that the bonding kinetics of Zdols on CHx is described by a time-dependent rate coefficient of the form $k(t) \propto k_o t^{-h}$, where $k(t)$ denotes the time-dependent rate coefficient, k_o is the initial rate constant, and h is the exponent that reflects the extent to which the bonding reaction is spatially confined.[13] For Zdols of similar molecular weight, the exponent h was found to vary from $0.5 \leq h \leq 1.0$ depending upon the stiffness of the main chain (as varied by changing the ratio of the perfluoromethylene oxide and perfluoroethylene oxide monomer units, Figure 1). The change in h therefore reflected the "melting" of the confined liquid from a solidlike ($h = 0.5$) to a liquidlike ($h = 1.0$) state. Here the temporal dependence of the bonding of ZDPA to CHx is found to be characteristic of diffusion-limited kinetics having the same $k(t) \propto k_o t^{-h}$ dependence. However, the bonding of ZDPA to CHx is characterized by $h \sim 0.25$, while Zdol of the same molecular weight and main chain structure bonds to the identical CHx with a $h = 1.0$ time dependence. The values for h indicate a significant difference in the degree of confinement of the adsorbed liquid film between ZDPA and Zdol. Both bonding and debonding rates are discussed. Model reactions between the alkylamine end group and possible surface polar functional groups are investigated via infrared studies and via ab initio quantum chemistry to provide insight into the specific nature of the intermolecular bonding reactions. The computed hydrogen bond strengths for some dimer interactions provide the basis for interpreting the observed kinetic data.

Experimental Section

Materials. The perfluoropolyether lubricants used in this work were obtained from Ausimont under the trade names Zdol 4000 and ZDIAC 2200. A sample of the dipropylamine-terminated ZDPA 4000 was kindly provided by P. Kasai and P. Brock of the IBM Almaden Research Center. Both Zdol 4000 and ZDPA 4000 are characterized by number-average molecular weights of ∼4100, a CF_2O/CF_2CF_2O monomer unit ratio of 1.1, and >99% end group functionalization as determined by NMR. Chemical structures are shown in Figure 1.

The substrates used in these studies were 95-mm-diameter rigid disks. These disks were comprised of a super-smooth AlMg substrate (RMS roughness of <15 Å) onto which were sputter-deposited an underlayer of Cr, a Cobalt-based magnetic layer, and nominally ∼100 Å of amorphous hydrogenated (CHx) carbon. The atomic composition of the carbon surface has previously been described.[13] The hydrogen incorporated into the carbon film was determined to be approximately 35 at. % as determined by Rutherford backscattering. The CHx films also contained 8 at. % oxygen, as determined by XPS (Phi Quantum 2000 ESCA system at a 75° takeoff angle).

Bonding Kinetics. The lubricants were applied to the disks from solutions of HFE-7100 (3M) using the dip-coat method. The lubricant film thicknesses were quantified using FTIR (Nicolet Model 560), calibrated to film thickness by XPS.[14] Throughout the following, we refer to the ZDPA and Zdol lubricants on the disk surface as being either "bonded" or "mobile." To clarify our definition of these terms, we briefly describe the methodology by which these quantities are determined. Following lubricant application, the initial lubricant thickness is measured via specular reflectance FTIR. The lubricated disks are then annealed for a specified period of time and the remaining lubricant film thickness remeasured. The decrease in the lubricant thickness following annealing yields the evaporated amount. In the following, we report the evaporated fraction which is defined as the amount evaporated normalized to the initial thickness. After annealing, the disks were washed sequentially in the hydrofluoroether HFE-7100 and 2,3-dihydro-perfluoropentane (Vertrel-XF, DuPont) solvents to remove any soluble lubricant, and the lubricant thickness was remeasured. The lubricant retained by the disk is defined to be the amount "bonded", while the portion removed by the solvent wash process is defined as the "mobile" lubricant. For bonded lubricant, our experiments do not distinguish between physi- and/or chemisorption. Again, the bonded and the mobile fractions are obtained by normalizing to the initial lubricant thickness.

Surface Energy Measurements. The surface energy as a function of ZDPA film thickness on CHx was determined from contact angle measurements using hexadecane ($\gamma_l^d \sim \gamma_l = 27.5$ mJ/m^2) and water ($\gamma_l^d = 21.8$ mJ/m^2 and $\gamma_l^p = 51.0$ mJ/m^2) as the reference liquids. The contact angle, θ, made

(10) (a) Scarati, A. M.; Caporiccio G. *IEEE Trans. Magn.* **1987**, *23*, 106. (b) Bargigia, G.; Gavezotti, P. *Poliplasti* **1992**, *420*, 138.

(11) Kondo, H. *Jpn. Kokai Tokkyo Koho* JP 07320255, 1995. See also *Chem. Abstr.* **1997**, *124*, 218362.

(12) Kasai, P. H.; Raman, V. *Tribol. Lett.* **2002**, *12*, 117.

(13) (a) Waltman, R. J.; Tyndall, G. W.; Pacansky, J.; Berry, R. J. *Tribol. Lett.* **1999**, *7*, 91. (b) Tyndall, G. W.; Waltman, R. J.; Pocker, D. *Langmuir* **1998**, *14*, 7527.

(14) Toney, M. F.; Mate, C. M.; Pocker, D. J. *IEEE Trans. Magn.* **1998**, *34*, 1774.

between a liquid and a solid surface is related to the free energy of the surface, γ_s, via Young's equation

$$\gamma_1 \cos\theta = \gamma_s - \gamma_{s1} \quad (1)$$

where γ_l is the surface energy (tension) of the reference liquid and γ_{sl} is the solid−liquid interfacial energy. The dispersive component of the surface energy is determined from contact angle measurements using reference liquids capable of interacting with the surface via dispersive forces only (i.e., hexadecane). In this case, the solid−liquid interfacial energy, γ_{sl}, is given by[15]

$$\gamma_{s1}^d = \gamma_s^d + \gamma_1^d - 2\sqrt{\gamma_s^d \gamma_1^d} \quad (2)$$

The dispersive component of the surface energy is then obtained by the substitution of eq 2 into eq 1,

$$\gamma_s^d = \frac{\gamma_1^d(1+\cos\theta)^2}{4} \quad (3)$$

When the reference liquid is capable of interacting with the surface via both dispersive and polar forces, the interfacial energy can be approximated by[15]

$$\gamma_{s1} = \gamma_s + \gamma_1 - 2\sqrt{\gamma_s^d \gamma_1^d} - 2\sqrt{\gamma_s^p \gamma_1^p} \quad (4)$$

which upon substitution into Young's equation readily provides an expression for the polar component of the surface energy.

Computational Methodology. Ab initio calculations were performed using the Gaussian 98 computer code.[16] All geometries were fully optimized using the density functional theory (DFT) at the 6-31G[d] and/or the 6-311++G[d,p] basis sets.[17] The DFT calculations employed Becke's 3-parameter functional together with Perdew and Wang's gradient-corrected correlation functional.[18,19] For all structures, differentiation of the energy gradients at the optimized geometries produced no imaginary frequencies. The molecular electronic properties are reported using the CHelpG population analyses.[20] Figures reproducing the computational results were made using the GaussView graphical user interface[21] and/or the CambridgeSoft graphical user interface.[22]

Results

1. Bonding Kinetics on CHx at Elevated Temperatures. The results of the bonding kinetic studies conducted on 10 Å of ZDPA 4000 and Zdol 4000 on amorphous hydrogenated carbon, CHx, between 64 and 150 °C and ≤4% relative humidity (RH) are compared in Figure 2. The two sets of data correspond to equivalent experiments conducted under identical conditions. Upon application of ZDPA 4000 and Zdol 4000 to the CHx surface, a small fraction (∼5−15%) of the lubricant bonds at room temperature within the time required to allow for solvent evaporation and to conduct the initial thickness measurements, Figure 2b,e. This quantity of bonded lubricant is referred to as the initial bonded fraction, while the quantity of lubricant that is not bonded to the CHx on the disk surface is referred to as the initial mobile fraction, Figure 2a,d. With increasing anneal time, the fraction of mobile ZDPA 4000 and Zdol 4000 present on the CHx surface decreases and is quantitatively accounted for by both the increase in the bonding of the lubricants to the CHx surface and the increase in the evaporation of the lubricants from the CHx surface, Figure 2c,f. At the anneal temperature of 64 °C, the loss of mobile lubricant due to evaporation is a minor reaction channel accounting for less than or equal to ∼5% of the total lubricant thickness loss. However, with increasing temperature, the loss of mobile lubricant due to the evaporation channel increases where at the maximum temperature of 150 °C, we observe an ∼10% loss of mobile lubricant from ZDPA 4000 and an ∼20% loss of mobile lubricant from Zdol 4000. On a comparative basis, there is less lubricant evaporation from ZDPA than from Zdol due to the more rapid bonding kinetics.

Figure 2 additionally indicates that ZDPA 4000 attains a considerably larger bonded fraction in a significantly shorter time than Zdol 4000 at all temperatures investigated. For example, at 64 °C, a 50% bonded fraction can be attained by ZDPA 4000 in ∼200 min compared to ∼3000 min for Zdol 4000. The data for ZDPA also shows that the bonding rate slows appreciably after approximately 80−90% bonded fraction is attained after which the data points deviate from the theoretical curves provided with the experimental data in Figure 2b. The discussion of this behavior is deferred to a later section. For now, the observed bonding kinetics for ZDPA on CHx is to be contrasted to the bonding kinetics exhibited by Zdol 4000 on CHx, which instead shows asymptotic behavior at long times that allows for a significant quantity of mobile lubricant to remain on the disk surface, Figure 2e.

Both the ZDPA and Zdol bonding rates shown in Figure 2 do not follow classical kinetics but instead are time-dependent with a rate coefficient that decreases with time. The theoretical fits accompanying the bonding data can be developed assuming a rate coefficient that is time-dependent, that is, $k(t) \propto k_o t^{-h}$, where $k(t)$ is the instantaneous rate coefficient at time t, k_o is the time-independent initial rate constant, and h is the coefficient describing the power function in time. Thus, the differential rate equations describing the depletion of mobile lubricant, A, the formation of bonded lubricant, B, and the evaporation of lubricant, C, may be written as

$$\frac{dB}{dt} = k(t)A = k_B t^{-h} A \quad (5)$$

$$\frac{dC}{dt} = k(t)A = k_C t^{-1} A \quad (6)$$

$$-\frac{dA}{dt} = \frac{dB}{dt} + \frac{dC}{dt} \quad (7)$$

(15) (a) Owens, D. K.; Wendt, R. D. *J. Appl. Polym. Sci.* **1969**, *13*, 741. (b) Kaelbe, D. H. *J. Adhes.* **1970**, *2*, 66.
(16) Frisch, M. J.; Trucks, G. W.; Schlegel, H. B.; Scuseria, G. E.; Robb, M. A.; Cheeseman, J. R.; Zakrzewski, V. G.; Montgomery, Jr., J. A.; Stratmann, R. E.; Burant, J. C.; Dapprich, S.; Millam, J. M.; Daniels, A. D.; Kudin, K. N.; Strain, M. C.; Farkas, O.; Tomasi, J.; Barone, V.; Cossi, M.; Cammi, R.; Mennucci, B.; Pomelli, C.; Adamo, C.; Clifford, S.; Ochterski, J.; Petersson, G. A.; Ayala, P. Y.; Cui, Q.; Morokuma, K.; Malick, D. K.; Rabuck, A, D.; Raghavachari, K.; Foresman, J. B.; Cioslowski, J.; Ortiz, J. V.; Baboul, A. G.; Stefanov, B. B.; Liu, G.; Liashenko, A.; Piskorz, P.; Komaromi, I.; Gomperts, R.; Martin, R. L.; Fox, D. J.; Keith, T.; Al-Laham, M. A.; Peng, C. Y.; Nanayakkara, A.; Gonzalez, C.; Challacombe, M.; Gill, P. M. W.; Johnson, B.; Chen, W.; Wong, M. W.; Andres, J. L.; Gonzalez, C.; Head-Gordon, M.; Replogle, E. S.; Pople, J. A. *Gaussian 98*, Revision A.7; Gaussian, Inc.: Pittsburgh, PA.
(17) McLean, A. D.; Chandler, G. S. *J. Chem. Phys.* **1980**, *72*, 5639.
(18) Becke, A. D. *J. Chem. Phys.* **1996**, *104*, 1040.
(19) Perdew, J. P.; Burke, K.; Wang, Y. *Phys. Rev. B* **1996**, *54*, 16533.
(20) Breneman, C. M.; Wiberg, K. B. *J. Comput. Chem.* **1990**, *11*, 361.
(21) *GaussView 2.1*; Gaussian, Inc.: Pittsburgh, PA.
(22) *CambridgeSoft Chem 3D Ultra*, Version 4.0; Cambridge, MA.

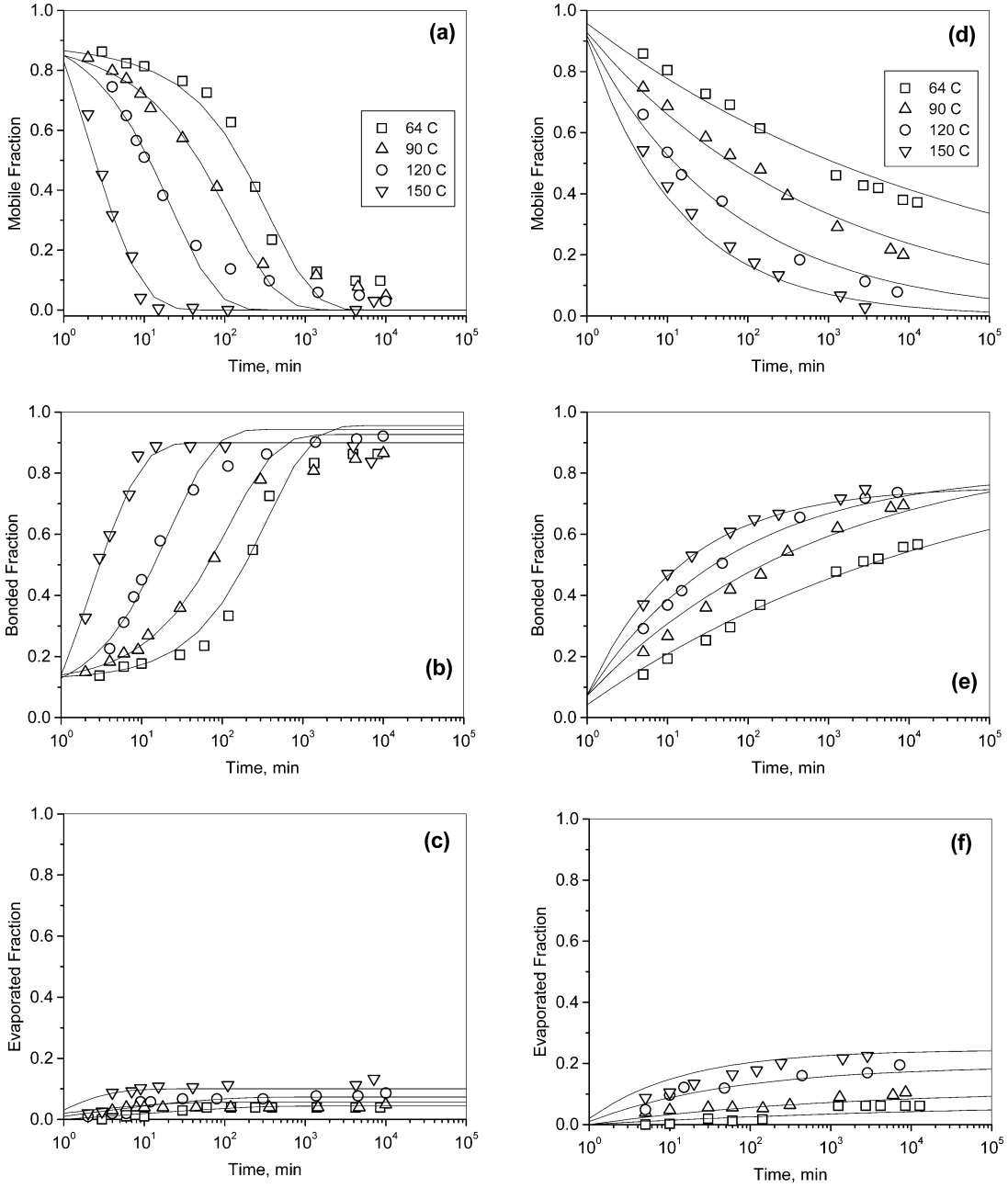

Figure 2. Changes in the mobile (a, d), bonded (b, e), and evaporated (c, f) fractions for (left) ZDPA-4000 and (right) Zdol 4000 on CHx (120 Å) as a function of time and temperature from 64 to 150 °C. All initial lubricant thicknesses were 10.5 ± 0.5 Å. The solid lines are the results of calculations derived from the theoretical rate law in eqs 5−7.

where k_B and k_C are the initial rate constants for bonding and evaporation, respectively. The results of the calculations based on this model are shown in Figure 2 as the solid lines. In all cases, the functional form of the time dependence in the evaporation channel, eq 6, follows an inverse time dependence in the differential rate equation. The origin of this inverse time dependence has been presented elsewhere.[23] Here, the focal point of the data presented in Figure 2 is that changing the end groups in an otherwise identical perfluoropolyether main chain can result in substantially different bonding kinetics on identical carbon surfaces. By an identical lubricant main chain is meant that both the molecular weight (MW) and the ratio of the perfluoromethylene- and perfluoroethylene-oxide monomer units making up the polymer backbone are the same; that is, for the latter, we are comparing lubricants with the same CF_2O/CF_2CF_2O or C1/C2 ratio. We have previously shown that the time dependence in the bonding kinetics is a strong function of the C1/C2 ratio in the perfluoropolyether backbone, which determines whether the perfluoropolyether behaves solidlike or liquidlike.[13] From a fit to the kinetic data shown in Figure 2 using eqs 5−7, we have determined that the bonding rate of Zdol 4000 and ZDPA 4000 on CHx follows $k(t) \propto k_B t^{-1.0}$ and $k(t) \propto k_B t^{-0.25\pm0.05}$, respectively. The kinetic data are summarized in Table 1.

As mentioned above, the changes in the mobile (or bonded) fraction for ZDPA at the longer times deviate

(23) Tyndall, G. W.; Waltman, R. J. *J. Phys. Chem. B* **2000**, *104*, 7085.

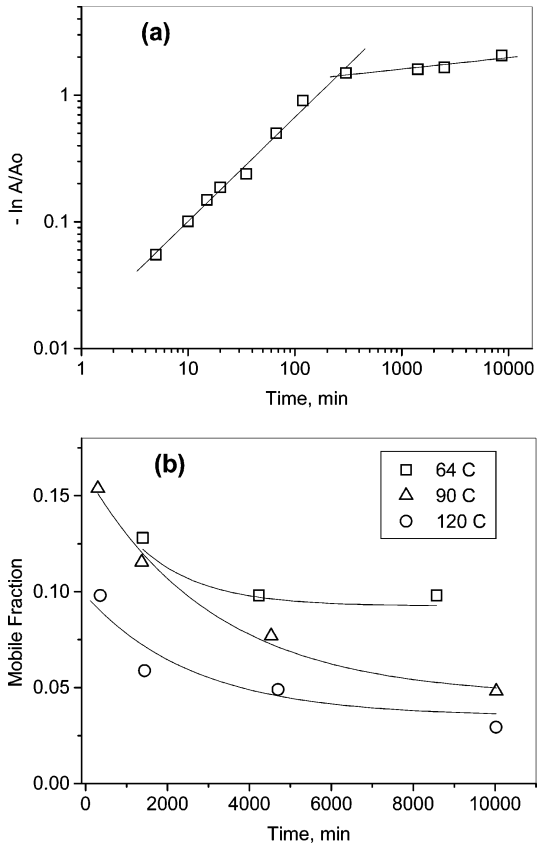

Figure 3. (a) Changes in the mobile fraction (A/Ao) of ZDPA-4000 on CHx as a function of time taken from the data shown in Figure 2a. At 64 °C, a "break" in the theoretical time dependence is observed at long times (greater than ~1000 min). (b) The solid lines drawn through the data points represent exponential fits to the data points over the time range indicated.

Table 1. Kinetic Data for the Bonding of Lubricants on CHx

lubricant	carbon	temperature, °C	h (t^{-h})	k_B	k_C
Zdol 4000	CHx	64	1.00	0.084	0.007
Zdol 4000	CHx	90	1.00	0.130	0.018
Zdol 4000	CHx	120	1.00	0.193	0.048
Zdol 4000	CHx	150	1.00	0.277	0.091
ZDPA 4000	CHx	64	0.23	0.007	0.010
ZDPA 4000	CHx	90	0.25	0.020	0.018
ZDPA 4000	CHx	120	0.20	0.064	0.019
ZDPA 4000	CHx	150	0.25	0.350	0.070

from the theoretical kinetic curves that are based strictly upon a $k(t) \propto k_B t^{-0.25}$ fit, Figure 2. For example, this deviation is readily visualized in Figure 3a where a "break" in the kinetics is observed for ZDPA at 64 °C for times greater than ~300 min. This longer time data may instead be fit to an exponential function, Figure 3b, which may be indicative that a "crossover" in the time dependence of the bonding kinetics has occurred. Crossovers to the exponential dependence have been observed in kinetic systems when finite volume effects begin to dominate the kinetic behavior via a macroscopic segregation of reactant pairs.[24]

2. Ambient Bonding and Debonding Kinetics on CHx. The results of the ambient bonding and debonding kinetic studies conducted on 11 Å of Zdol 4000 on CHx and 10−12 Å of ZDPA 4000 on CHx at 20 °C and either 0% relative humidity (RH) or 50% (RH) are presented in Figure 4. Both the bonding and debonding kinetics for each respective lubricant is presented on a single plot to allow the determination of the equilibrium bonded fraction over the time range indicated. In the debonding experiments, the rate of debonding for each lubricant is followed as a function of time using initially 100% bonded lubricant on the carbon surfaces. These disks are produced by annealing the applied lubricant for a suitable period of time based upon the bonding and evaporation kinetics as typically shown in Figure 2. The annealing temperature is selected to minimize evaporative loss (~5−10%) which could otherwise change the molecular weight (MW) distribution of the remaining bonded lubricant and possibly influence the debonding kinetics. Immediately after annealing, the disks are rinsed with solvent (Vertrel-XF) to produce the 100% bonded disks. These disks are then measured for lubricant thickness before and after solvent rinse as a function of time. With increasing time, the fraction of bonded lubricant that can be removed by the solvent increases, indicating that some of the bonded lubricant has been converted to mobile lubricant. We assume that the bonded lubricant is displaced by the water that is adsorbed on the disk surface. This assumption is verified by conducting the following experiments: (i) when the disks with the bonded lubricant are placed in a dry environment (i.e., 0% RH), there is no net displacement

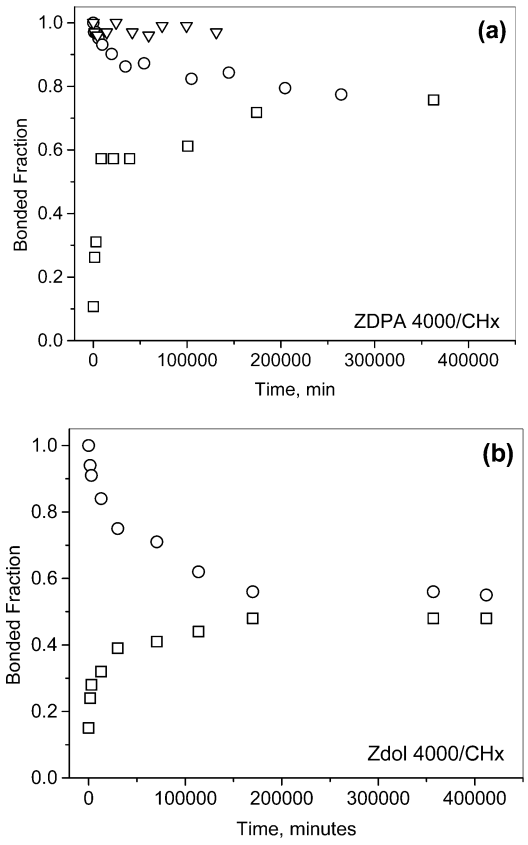

Figure 4. Changes in the bonded fractions for (a) ZDPA 4000 and (b) Zdol 4000 on CHx as a function of time at 21 °C. (a) Bonding for 12.0 ± 0.5 Å (□) and debonding for 10.0 ± 0.5 Å (○) at 50 ± 10% relative humidity (RH), and debonding for 10.0 ± 0.5 Å (▽) at 0% RH. (b) Bonding for 12.0 ± 0.5 Å (□) and debonding for 10.0 ± 0.5 Å (○) at 50 ± 10% RH.

(24) (a) Argyrakis, P.; Kopelman, R.; Lindenberg, K. *Chem. Phys.* **1993**, *177*, 693. (b) Lindenberg, K.; Argyrakis, P.; Kopelman, R. *J. Phys. Chem.* **1995**, *99*, 7542. (c) Ovchinnikov, A. A.; Zeldovich, Y. B. *Chem. Phys.* **1978** *28*, 215.

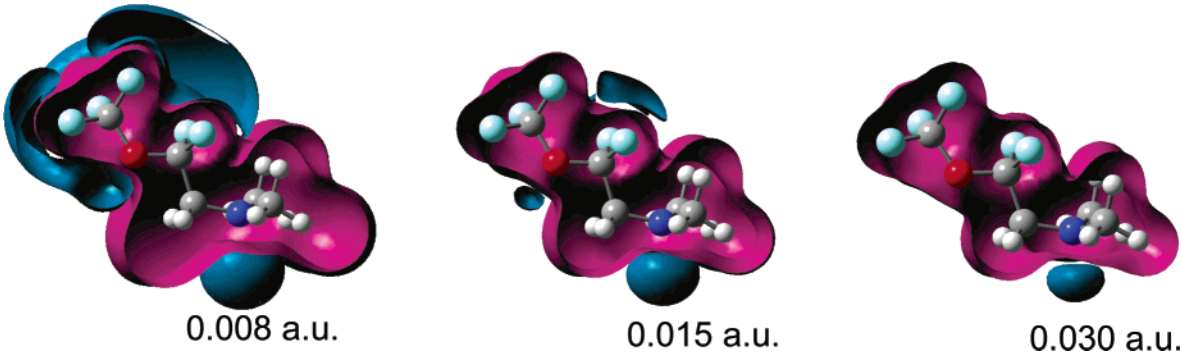

Figure 5. Computed electrostatic potentials (ESP) as a function of isosurface for the B3PW91/6-31G[d] optimized geometry of a model ZDPA molecule.

of the bonded lubricant, Figure 2a; and (ii) when the disks with the bonded lubricants are immersed in boiling water, all of the bonded lubricant can eventually be removed. Thus, the equilibrium reaction can be described by eqs 8 and 9 below:

$$A \xrightarrow{k(t)} B \tag{8}$$

$$B + H_2O \xrightarrow{k'} A \tag{9}$$

where A and B represent the mobile and bonded lubricants, respectively. At equilibrium, the forward (eq 8) and reverse (eq 9) rates are equal:

$$\frac{\text{rate}_{\text{forward}}}{\text{rate}_{\text{reverse}}} = \frac{[B]\,[H_2O]}{[A]} \tag{10}$$

Therefore, an increase in the concentration of water [H_2O] will drive an increase in mobile lubricant [A] or, equivalently, a decrease in the bonded lubricant [B]. At 50% RH, there is enough adsorbed water on the disk surface to drive the reverse reaction debonding for both (fully bonded) Zdol 4000 and ZDPA 4000 on CHx to their equilibrium bonded fractions. In Figure 4b, we observe for Zdol 4000 that both the bonding and debonding data converge to an equilibrium bonded fraction of ~40−50% over the time range indicated. This is to be contrasted to Figure 4a where under identical conditions we observe that ZDPA converges to a comparatively higher equilibrium bonded fraction of ~75−80% over the time range indicated. Regarding ambient bonding, ZDPA attains 50% bonded fraction in $\sim 10^3$ min compared to $\sim 10^5$ min for Zdol 4000 due to the different kinetic time dependencies. Therefore, the kinetic data are indicative that ZDPA has not only a much higher bonding rate than Zdol on CHx but also a higher equilibrium bonded fraction over 10^6 min. Also, debonding indicates that water can compete with the lubricant for the same polar sites on the carbon surface.

3. ZDPA Reactivity. The bonding observed for ZDPA on CHx is energetically driven by the reactive dialkylamine end groups.[25] Aliphatic tertiary amines are considerably more basic than primary alcohols; consequently, they are reactive with acid groups and capable of hydrogen bonding to polar sites on the carbon surface as well as to polar contaminants such as water. The computed electrostatic potential for ZDPA provides a measure of the reactivity of ZDPA by showing the charge distribution in the molecule. In Figure 5, the blue-colored regions represent excess negative charge, and the red-colored regions indicate excess positive charge. To keep the computations tractable, CF_3OCF_2-$CH_2N(CH_3)_2$ is used as the model structure for the ZDPA lubricant. Since the electrostatic potential is sampled over the entire accessible surface of the model lubricant, corresponding roughly to a van der Waals contact surface, the figure shows that the nitrogen atom in the ZDPA end group accumulates considerable negative charge, thereby identifying the most likely interaction site for the bonding reaction to the carbon surface. This is determined from the series of figures which show that as the interaction energy is increased from 0.008 to 0.030 au (atomic units), the excess negative charge is increasingly isolated on the amine nitrogen atom. Frontier molecular orbital analyses indicate that the molecular orbital housing the nonbonding lone pair of electrons that reside in a p-orbital on the ether oxygen atom is energetically buried 3.3 eV beneath the nitrogen lone pair of electrons (highest occupied molecular orbital) and therefore not as available for bonding interactions.

4. ZDPA Reactivity with Carboxylic Acid. To assess the possible bonding interactions between the amine end group in ZDPA and the CHx surface, we have first investigated the reaction between ZDPA and ZDIAC, the latter a carboxylic acid-terminated perfluoropolyether shown previously in Figure 1. ZDIAC was chosen as a reactant to ZDPA for several reasons. First, the CHx surface contains polar functional moieties such as carboxylic acids and hydroxyls.[26] Second, the reaction can be readily studied in the bulk since the two liquids are mutually soluble. The results of these studies are shown in Figure 6. Figure 6a shows the (transmission) infrared spectrum of each lubricant before they are mixed. ZDIAC shows the characteristic C═O stretching vibration at 1775 cm^{-1} due to the carboxylic acid end group. Figure 6b shows the infrared spectrum of an approximately equimolar mixture of ZDPA and ZDIAC shortly after mixing the two lubricants. The intensity of the ZDIAC carbonyl C═O stretch is significantly reduced with the concomitant formation of a new absorption band at 1673 cm^{-1}, which is attributed to the carbonyl C═O stretch of the carboxylate anion due to the formation of the NH^+COO^- salt.[27] Since the bulk

(25) Hussein, M. A.; Millen, D. J. *Faraday Trans. 2* **1974**, *70*, 685. Tollenaere, J. P.; Moereels, H. *Tetrahedron Lett.* **1978**, *15*, 1347.

(26) Zadowski, J. In *Chemistry and Physics of Carbon*, Vol. 21; Walker, P. L., Ed.; Dekker: New York, 1988.

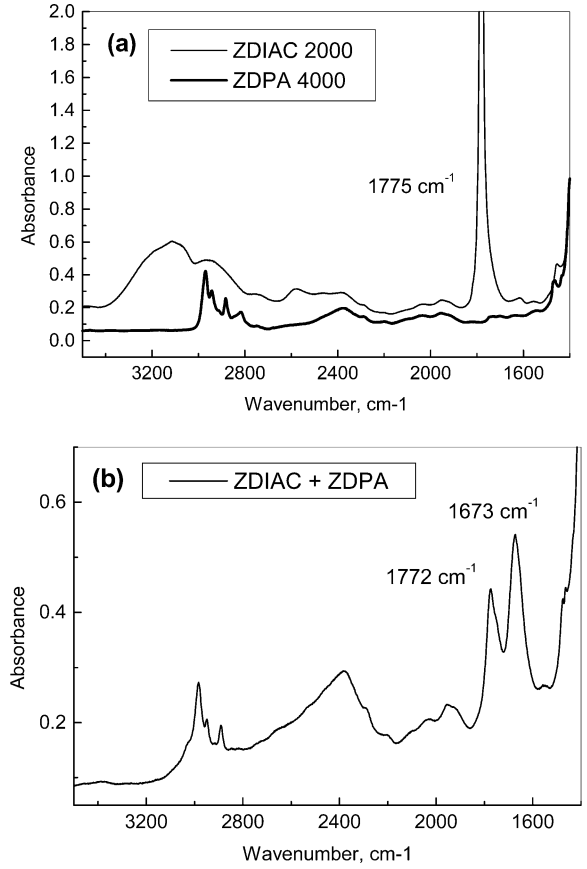

Figure 6. (a) Transmission infrared spectra of bulk (0.029-mm path length) ZDPA 4000 and ZDIAC 2000 before mixing at 20 °C. (b) The infrared spectrum of a mixture of ZDPA 4000/ZDIAC 2000 (2:1 weight ratio) at 20 °C within the time required for mixing and recording the spectrum (<10 min).

reaction between the amine and acid end groups proceeds spontaneously, we might infer that the rapid bonding observed for ZDPA on CHx may in part be a manifestation of such energetically favorable reaction pairs.

5. ZDPA Hydrogen-Bonding Interactions. In addition to the presence of polar functional groups such as carboxylic acid on CHx, there are other polar groups on the carbon surface that can also provide the weaker but still significant hydrogen bonding. The hydrogen-bonding interactions between amines and alcohols are well-investigated.[28] Hydrogen-bonding interactions for the ZDPA and Zdol lubricants with a possible surface polar group such as the hydroxyl are investigated here via ab initio computations on model dimers. The optimized geometries and computed energetics for some dimer interactions are summarized in Table 2 and Figure 7. We begin first with a brief description of the optimized geometries of the hydrogen-bonded dimers followed by a discussion of their binding energies. In these studies, the amine end group in ZDPA will act as a base (electron donor) while the hydrogen atom in the hydroxyl end group of Zdol will act as the proton donor. The latter is a manifestation of gas-phase calculations where the lubricant alcohol end group, in the absence

Table 2. Ab Initio Computed Optimized Geometries and Energetics for the Intermolecular Interactions between Lubricant and Surface Models[a]

reaction	ΔE, kcal/mol 6-311++G[d,p]	R_{xy}, Å 6-311++G[d,p]
Figure 7a: ZDPA, CH_3OH	−4.35	2.882
Figure 7b: Zdol, CH_3OH	−5.29	2.798
Figure 8: Zdol dimer	−4.60	2.843

[a] The reactants and dimers are structurally optimized at B3PW91 using the 6-311++G[d,p] basis set. All optimized geometries had no computed imaginary frequencies. ΔE represents the difference in total energies corrected for zero-point energies. R_{xy} represents the interatomic distance between X and Y in the H-bond, X−H---Y.

of solvation effects, will act as a stronger acid than either water or an alkyl alcohol. The binding energy is obtained as the difference between the total energies of the dimer and the isolated reactants, that is, $\Delta E = E_{AB} - (E_A + E_B)$, corrected for zero-point energy contributions. We note that the computed H-bond (hydrogen bond) energy for the various dimers are reported at the 6-311++G(d,p) basis set which, in addition to including the diffuse functions important in describing systems with lone pair of electrons, also include the hydrogen atom *p* functions, both of which are important in quantitatively describing hydrogen bonding. We expect the results of these calculations to be very close to the Hartree−Fock limit.[29]

Figure 7a presents the optimized geometry for the hydrogen-bonded dimer of ZDPA with CH_3OH. The CH_3-OH represents a hydroxyl-terminated carbon surface group. The equilibrium H-bond distance between the amine nitrogen atom and the −OH hydrogen atom is 1.92 Å. The H-bond energy for the $CHF_2CH_2N(CH_3)_2$−CH_3OH dimer is $\Delta E = -4.35$ kcal/mol. Figure 7b also shows the hydrogen-bonded dimer between Zdol and CH_3OH. The H-bond distance is 1.83 Å, and the hydrogen bond strength is −5.29 kcal/mol, somewhat larger than that for the ZDPA−CH_3OH dimer. The computed binding energies are consistent with what has previously been reported in similar dimer systems.[30,31] The greater radial extent of the ZDPA amine N---H−O hydrogen bond compared to the Zdol hydroxyl H---O(H)-CH_3 is attributed to the lower nuclear charge on the nitrogen atom.

Discussion

The bonding of molecularly thin perfluoropolyether lubricant films to amorphous carbon surfaces is energetically driven by the decrease in the free energy that results from the interaction of the polar functional end groups (i.e., alcohol, dialkylamine) with the polar sites on the carbon surfaces.[13,14] For both ZDPA and Zdol, the computed H-bond energy is on the order of 5 kcal/mol when surface hydroxyl groups are involved (Table 2). Stronger interactions such as the formation of the NH^+COO^- salt appear to be possible for the ZDPA amine end group with the carboxylic acid group based upon IR studies of bulk solutions. However, the surface

(27) Colthup, N. B.; Daly, L. H.; Wiberley, S. E. *Introduction to Infrared and Raman Spectroscopy*; Academic Press: New York, 1990; p 317.
(28) Saikia, B.; Suryanarayana, I.; Saikia, B. K.; Haque, I. *Spectrochim. Acta* **1991**, *47A*, 791.
(29) Hankins, D.; Moskowitz, J. W.; Stillinger, F. H. *J. Chem. Phys.* **1970**, *53*, 4544.
(30) Hirano, E.; Kozima, K. *Bull. Chem. Soc. Jpn.* **1966**, *39*, 1216.
(31) Kramer, R.; Zundel, G. *J. Chem. Soc., Faraday Trans.* **1990**, *86*, 301.

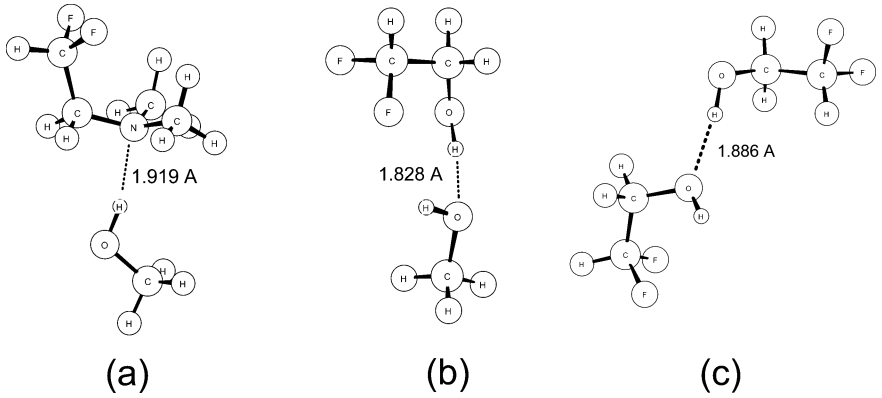

Figure 7. B3PW91/6-311++G(d,p) optimized geometries for some model interactions of (a) ZDPA and (b) Zdol with a possible surface −OH hydroxyl group, and (c) Zdol−Zdol. The equilibrium intermolecular distances between the model lubricant end groups and the surface polar group are given in Å.

bonding reaction can be kinetically constrained if it is diffusion-limited or if the bonding has an activation energy for reaction. These barriers arise from the ability of the lubricant molecules to spatially deliver the polar functional end groups (i.e., hydroxyl, dialkylamine) to the active sites on the carbon surfaces, or from the energetic requirements of the activation barrier along the bonding potential energy surface. Diffusion-limited kinetics are additionally affected by the spatial dimension in which they occur and can exhibit nonclassical reaction kinetics that are manifested by a time-dependent rate coefficient. The time dependence originates from the fact that diffusion is not an effective self-stirring mechanism in low dimensions, giving rise to a segregation of reactant pairs as the reaction proceeds.[32] In these studies we observe that despite the energetic driving force for the bonding of the lubricant end groups to the carbon surface, the bonding of both ZDPA and Zdol on CHx are kinetically limited, having a time-dependent rate coefficient of the general form $k(t) \sim t^{-h}$.

The experimental data presented in Figures 2 and 4 are indicative that the bonding rate follows the order ZDPA/CHx > Zdol/CHx. Since only the functional end groups are different between ZDPA and Zdol, Figure 1, the surprising and rather significant differences in the bonding kinetics must be attributable to the different end groups and their cohesive and/or adhesive interactions. The bonding kinetics shows that the amine end groups are reactive to the CHx surface and possible adhesive interactions have already been discussed. From the computed binding energies (Table 2) and the model surface reaction (Figure 6), we assume that when the distance between a ZDPA end group and a carbon surface site becomes smaller than the "capture" radius, a bonding reaction takes place. The survival probability of the reactant (e.g., ZDPA as the moble lubricant) is therefore dependent upon the density of trapping sites[33] and the mean number of distinct sites it can visit before encountering the trap.[34] We now discuss how the hydroxyl and dipropylamine end group structures could impact the survival probability and therefore the bonding kinetics of the lubricants on CHx.

There are several major differences between the dipropylamine and hydroxyl end groups that may impact the bonding kinetics. First, the tertiary amine end groups in ZDPA do not self-associate as indicated by the infrared spectrum in Figure 6a, which could possibly allow the amine end groups in ZDPA to form more lubricant/carbon reactant pairs initially. Second, the propyl end groups can associate with the underlying CHx surface, possibly allowing the dipropylamine end groups to be located preferentially nearer to the carbon surface. Third, as discussed previously, the greater radial extent of the amine nitrogen lone pair (Figure 7) could also allow for a more facile exploration of the carbon surface by the lubricant, that is, a larger capture radius. While we have no way of quantifying the significance of the latter on the bonding kinetics at this time, the lack of self-association between ZDPA molecules can be compared to the hydroxyl end groups in Zdol which can form intermolecular Zdol−Zdol hydrogen bonds. The Zdol end groups may therefore act as additional trapping sites that compete for Zdol−CHx bonding. The computed binding energy for such a Zdol dimer, Figure 7c, is $\Delta E = -4.60$ kcal/mol (Table 2). The results of the computations show that there could still be a net driving force for the bonding of a Zdol hydroxyl end group to, say, CH_3OH ($\Delta E_{rxn} = -0.69$ kcal/mol). More importantly, the Zdol−Zdol trap ($\Delta E = -4.60$ kcal/mol) will compete energetically for the Zdol−CH_3OH dimer ($\Delta E = -5.29$ kcal/mol), possibly reducing the bonding rate in the Zdol/CHx system.

The possible increased density of ZDPA−carbon reactant pairs that are initially formed on the CHx surface as a consequence of the dipropylamine end groups is further considered by the measurement of the surface energies for ZDPA on CHx as a function of the lubricant film thickness. We stress that these measurements were completed within ∼10−15 min of lubricant application to characterize the state of the adsorbed lubricant film at the start of the bonding kinetics experiments such as that presented in Figure 2. The dependence of both the dispersive (γ_s^d) and polar (γ_s^p) surface energies as a function of ZDPA film thickness is presented in Figure 8. The dispersive component of the surface energy, γ_s^d, is observed to decrease monotonically with increasing lubricant thickness from 0 to 15 Å. γ_s^d then increases as the film thickness is increased over the range from 15 to 25 Å. Thus, a minimum in γ_s^d is observed near 15 Å.

(32) (a) Kopelman, R. In *The Fractal Approach to Heterogeneous Chemistry*; Avnir, D., Ed.; John Wiley & Sons Ltd.: Chichester, UK, 1989; pp 295−309. (b) Kopelman, R. *Science* **1988**, *241*, 1620.

(33) Lin, A. L.; Monson, E.; Kopelman, R. *Phys. Rev. E* **1997**, *56*, 1561.

(34) Kopelman, R. *J. Stat. Phys.* **1986**, *42*, 185.

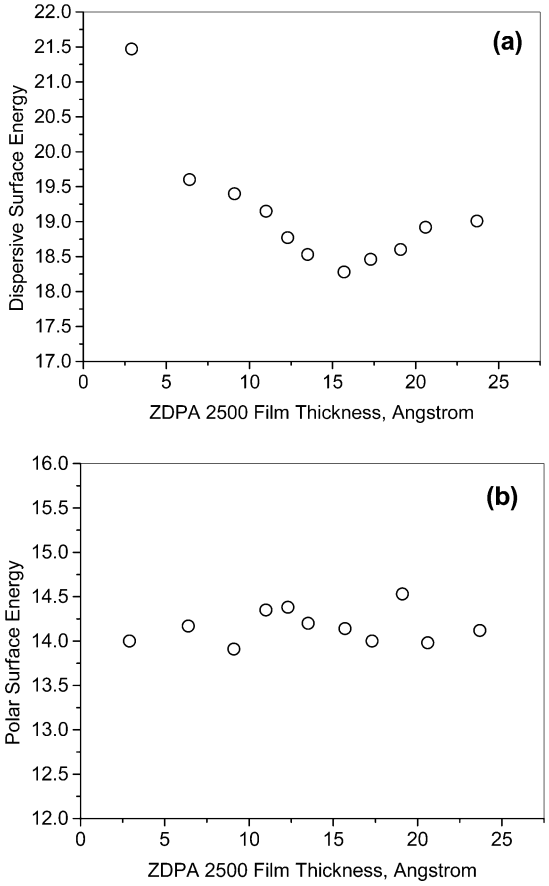

Figure 8. (a) Dispersive and (b) polar surface energies as a function of ZDPA 2500 film thickness on CHx. The surface energy units are in erg/cm^2.

The absence of an analogous minimum in the Zdol/CHx system[14] is indicative that the dipropylamine end group is preferentially located near the CHx surface compared to the perfluoropolyether backbone for film thicknesses <15 Å. (The minimum in γ_s^d also defines the monolayer thickness for ZDPA 2500 on CHx.) In contrast, the polar component of the surface energy, γ_s^p, shows no clear surface energy minimum immediately after application of the lubricant film but instead shows a surface energy of ~14 mJ/m^2 that is fairly invariant as a function of film thickness. This is characteristic of ZDPA that has not formed any significant polar adhesive interactions to the CHx surface. This is further corroborated by measurement of the bonded fraction of ZDPA on CHx immediately after the surface energy measurements are made, which, as shown in Table 3, is less than or equal to ~7%. These data are consistent with the interpretation that the dipropylamine end groups within the first monolayer are closer to the CHx surface even if the amine nitrogen atom has not necessarily bonded to a CHx polar site.

If a higher density of reactant pairs is initially formed by the ZDPA−carbon couple and the initial bonding rate is higher, then the bonding of ZDPA to the carbon surface can lead to a nonrandom distribution of reactant pairs. The observed $k(t) \sim t^{-0.25}$ time dependence is indicative of such a rapid reaction that leads to the segregation of ZDPA−carbon pairs which then cannot be readily replenished by self-diffusive stirring on the disk surface. As the macroscopic segregation becomes on the order of the film thickness, finite volume effects

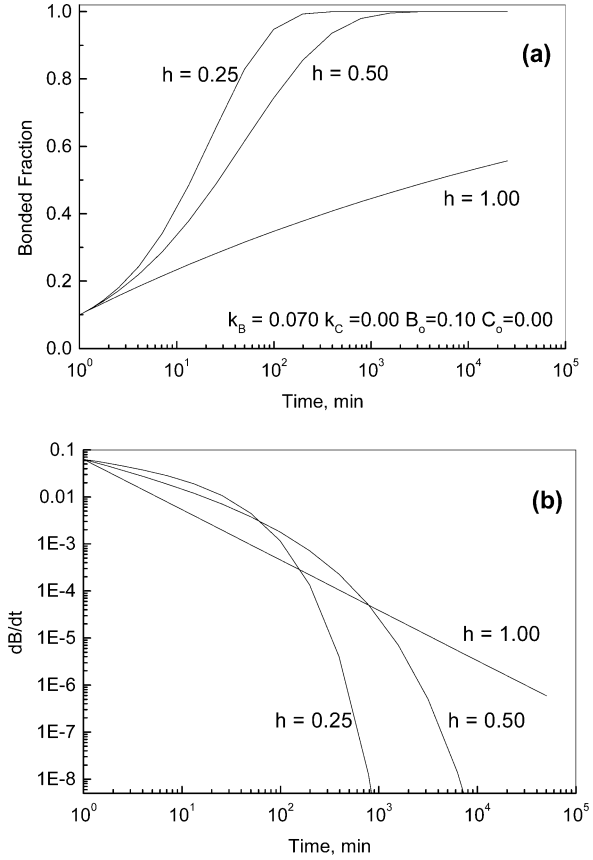

Figure 9. Computed changes in the integrated (top) and differential (bottom) bonding kinetics based upon eqs 5−7. In all simulations, the same bonding rate constant $k_B = 0.07$, evaporation rate constant $k_C = 0.00$, initial bonded fraction $B_o = 0.10$, and initial evaporated fraction $C_o = 0.00$ were used.

Table 3. ZDPA 2500 Total and Bonded Film Thicknesses for the Data Presented in Figure 8

total thickness, Å	bonded thickness, Å	bonded fraction
2.9	0.2	0.07
6.4	0.3	0.05
9.1	0.4	0.04
11.0	0.4	0.04
12.3	0.5	0.04
13.5	0.8	0.06
15.7	0.8	0.05
17.3	0.7	0.04
19.1	0.7	0.04
20.6	0.7	0.03
23.7	0.8	0.03

dictate the longer time reaction kinetics as previously discussed in the presentation of Figures 2 and 3. Further elaboration of the bonding kinetics is now considered in Figure 9. The bonding kinetics are simulated using eqs 5−7 and assuming that the rate coefficient is given by $k(t) \sim t^{-h}$; that is, no crossover in the time dependence is explicitly considered. Figure 9a plots the expected bonded fraction as a function of time showing the effect of the power exponent on the computed bonding kinetics. Figure 9b plots the rate of change of the bonded fraction as a function of time. From these plots it becomes evident that as the time exponent h decreases from 1.00 to 0.25, the initial bonding rate increases. For example, after 10 min, dB/dt for $h = 0.25$ is ~10 times larger than that for $h = 1.00$. However, with increasing time, Figure 9b shows that the bonding rate dB/dt decreases more quickly with

decreasing h, a manifestation of the segregation (depletion zone) between reactant pairs. The monotonic decrease computed for dB/dt for $h = 1.00$ is attributed to bonding kinetics that occurs from a more liquidlike film that is more capable of replenishing reactant pairs;[13] hence, the sharp drop-off in dB/dt is not observed for $h = 1.00$.

The nitrogen lone pair of electrons in ZDPA that is involved in the hydrogen-bonding reactions to the surface groups occupies one corner of a tetrahedral as a result of the sp^3 orbital configuration. Since the nitrogen lone pair of electrons cannot maintain enantiomeric configuration except possibly in the most hindered of structures, there is rapid inversion of the lone pairs about the nitrogen atom. While the energetic barrier for nitrogen inversion is generally low, ~3−8 kcal/mol, the inversion is often in competition with or accompanied by rotation(s) about the carbon−nitrogen bond whose energy barrier can be smaller than that of the inversion itself.[35,36] The inversion between two pyramidal configurations of ZDPA is explicitly considered in Figure 10. The transition state to the inversion barrier is computed to be only ~3 kcal/mol. Therefore, the spatial delivery of the nitrogen lone pair of electrons to within the capture radius of the surface polar site could be facilitated over bond rotations along the perfluoroether main chain as would otherwise be required of Zdol.[13]

Conclusions

The studies presented herein have demonstrated the significant impact that the lubricant end group can have on the bonding to amorphous carbon surfaces. We have attempted to identify the major differences between the hydroxyl and the dipropylamine end groups that may impact the bonding kinetics on amorphous carbon surfaces. The bonding kinetics of the dipropylamine-terminated ZDPA 4000 to a CHx surface was found to be time-dependent with a generalized rate coefficient given by $k(t) \propto k_B t^{-h}$. The initial bonding rate for ZDPA was found to be significantly greater than that for Zdol 4000, with ZDPA exhibiting a $t^{-0.25}$ time dependence compared to a $t^{-1.0}$ time dependence for Zdol 4000. The bonding kinetics were attributed to the reactivity of the amine end group, and the higher initial density of reactant pairs in the ZDPA/CHx system. The higher initial density of reactant pairs was suggested based upon the minimum in the dispersive surface energy of ZDPA as a function of film thickness, and the relatively low inversion barrier centered about the amine end group. Thus, a change in the functional end group of an otherwise identical Zdol main chain produced a lubricant whose bonding kinetics was significantly different from Zdol.

We have also presented data showing that bonded lubricant, both Zdol and ZDPA, can debond to replenish mobile lubricant. The debonding is driven by displacement by water. Thus, while at low relative humidity and elevated temperatures, 100% bonded fraction on the disk surface can be attained, bonding can be inhibited, and/or debonding can occur at the higher humidities.

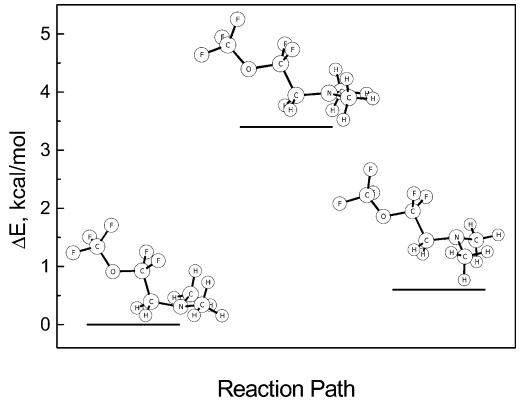

Figure 10. B3PW91/6-31G[d] optimized geometries and activation energy for the inversion of the nitrogen atom between the two pyramidal geometries. The total energies are corrected for zero-point energy contributions. The invertomer has a single imaginary frequency (233i cm^{-1}) associated with the interconversion between the two pyramidal geometries.

CM030065B

(35) Casarini, D.; Lunazzi, L.; Anderson, J. E. *J. Org. Chem.* **1993**, *58*, 714.
(36) Bushweller, C. H.; Fleischman, S. H.; Grady, G. L.; McGoff, P.; Rithner, C. D.; Whalon, M. R.; Brennan, J. G.; Marcantonio, R. P.; Domingue, R. P. *J. Am. Chem. Soc.* **1982**, *104*, 6224.
(37) Tyndall, G. W.; Waltman, R. J.; Pacansky, J. *J. Appl. Phys.* **2001**, *90*, 6287.
(38) Shukla, N.; Gellman, A. J.; Ma, X.; Gui, J. *Tribol. Lett.* **2002**, *12*, 105.